Electromagnetic theory of the coupling of zero-dimensional exciton and photon states: A quantum dot in a spherical microcavity

M. A. Kaliteevski
Department of Physics, University of Durham, South Road, Durham DH1 3LE, United Kingdom and Groupe d'Edude des Semiconducteur, CC074 Universite de Montpellier II, Place Bataillon, 34095 Montpellier Cedex 05, France

S. Brand and R. A. Abram
Department of Physics, University of Durham, South Road, Durham DH1 3LE, United Kingdom

V. V. Nikolaev
Ioffe Physicotechnical Institute, Polytschnicheskaya, 26, St. Petersburg, Russia and School of Physics, University of Exeter, Stocker Road, Exeter EX4 4QL, United Kingdom

M. V. Maximov and C. M. Sotomayor Torres
Institute of Material Science and Department of Electrical Engineering, University of Wuppertal, Gauss-Strasse 20, 42097 Wuppertal, Germany

A. V. Kavokin
LASMEA, UMR6602 du CNRS, Universite Blaise Pascal-Clermont-Ferrand II, 63177 Aubiere Cedex, France
(Received 25 January 2001; published 24 August 2001)

Exciton-light coupling in spherical microcavities containing quantum dots has been treated by means of classical electrodynamics within the nonlocal dielectric response model. Typical anticrossing behavior of zero-dimensional exciton-polariton modes has been obtained, as well as the weak-coupling-strong-coupling threshold. The influence of the cavity *Q* factor on the optical response of the structure has been analyzed.

DOI: 10.1103/PhysRevB.64.115305 PACS number(s): 42.55.Sa, 73.21.La

I. INTRODUCTION

Exciton-light interactions have been a subject of growing interest since the 1950s, when the concept of exciton polaritons was originally formulated by Hopfeld[1] and Agranovich.[2] An exciton polariton is a quasiparticle combining the properties of an electronic excitation and a light wave. Exciton polaritons can play a major role in the low-temperature optical properties of semiconductor structures and exhibit a remarkable variety of properties that are mostly dependent on the dimensionality of the system.

Bulk exciton polaritons have been studied experimentally in semiconductor films since the 1970s (see, e.g., Refs. 3 and 4). The epoch of quantum wells (QWs) started in the 1980s and revealed the crucial influence on the properties of exciton polaritons of the dimensionality of the excitonic state that was coupled to the light. The semiclassical theory of exciton polaritons in QWs and superlattices was developed by a number of workers, including Andreani *et al.*[5] and Ivchenko.[6] At the beginning of the 1990s, the rapid development of molecular-beam epitaxy allowed further reduction of the dimensionality of both the exciton and photon states forming the exciton polaritons. High-quality quantum wire and quantum dot (QD) structures are now widely studied by different experimental techniques, including time-resolved optical spectroscopy, which can give information on the kinetics of exciton polaritons in these structures.[7,8] The basic principles of the semiclassical description of these systems have been formulated[9,10] and are currently being applied to predict the behavior of structures of topical interest.

Since the first report of the strong coupling in quantum microcavities by Weisbuch *et al.*,[11] a huge number of papers devoted to exciton polaritons in planar microcavities have appeared. Strong enhancement of the light-matter coupling strength in these structures has been demonstrated, both experimentally and theoretically (e.g., Ref. 12 and references therein). A further decrease of the dimensionality of the photonic state coupled to the exciton is possible in pillar microcavities[13,14] and spherical Bragg microcavities.[15] Recent progress in photonic crystal fabrication gives hope that the four-decade-long progression to lower dimensionality in exciton-polariton systems will soon achieve its logical conclusion with the appearance of photonic dots with embedded electronic quantum dots. In particular, technological advances in the fabrication of spherical objects by the techniques of colloidal chemistry,[16,17] and other methods[18] will hopefully provide a means for the practical fabrication of multilayered structures of spherical symmetry in due course.

A rigorous theoretical analysis of an ideal system that exhibits coupling of zero-dimensional photons with zero-dimensional excitons seems timely.

We consider an ideal spherical QD embedded in an ideal spherical microcavity (SMC), as shown in Fig. 1, and we use the Green-function approach for quantum dots proposed by Banyai and Koch.[10] The fact that it is possible to obtain an analytical solution of the polariton eigenmode equation makes this model system especially attractive for a theoretical study.

The essential difference between our model system and that considered by Andreani *et al.*[14] is that we restrict our

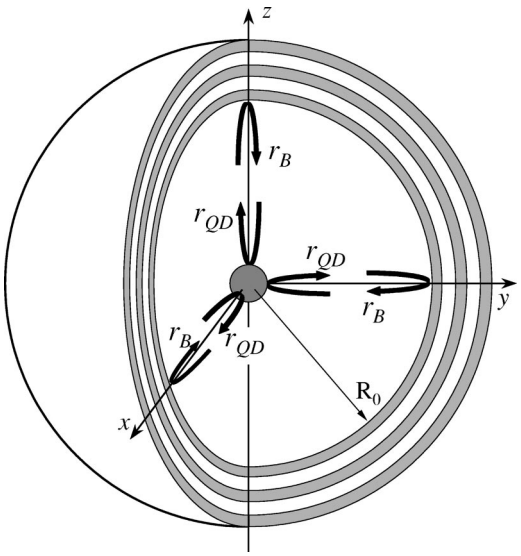

FIG. 1. A schematic diagram of a spherical microcavity with a quantum dot at its center. A central core of radius R_0 with the refractive index n_0 is surrounded by a spherical Bragg reflector, constructed from alternative layers of refractive indices n_1 and n_2 .

attention to a system having a spherical symmetry, rather than one of cylindrical symmetry.[14] As will be shown below, these two cases show quite important differences in behavior. We also demonstrate the distinctive features of zero-dimensional (spherical) exciton polaritons compared to conventional polaritons formed by plane light waves.

II. BASIC EQUATIONS

A. Reflection of the spherical light wave by a quantum dot

A spherical electromagnetic wave can be represented as a superposition of two waves with decoupled polarizations:[19] a TE wave with components $H_r, E_\theta, E_\phi, H_\theta, H_\phi$, and a TM wave with components $E_r, E_\theta, E_\phi, H_\theta, H_\phi$. Here E and H denote the electric and magnetic fields, respectively. The spatial dependence of the electric and magnetic fields in a spherical wave can be expressed in terms of spherical harmonics characterized by a positive integer l and an integer m in the interval from $-l$ to l, which are related to the angular orbital momentum and its projection. The value $l=0$ corresponds to a fully spherically symmetric electromagnetic wave, which does not exist for nonzero frequency.[15,19] In the case of the TE polarization, the spherical wave field with frequency ω in a medium with dielectric constant ε can be written as

$$\vec{E}_{l,m} = -\mu k_0 \left(\frac{m}{\sin\theta} P_l^{|m|}(\cos\theta)\vec{e}_\theta + i\frac{\partial}{\partial\theta} P_l^{|m|}(\cos\theta)\vec{e}_\phi \right) \times V(r)\exp(im\phi), \tag{1a}$$

$$\vec{H}_{l,m} = \left\{ \frac{l(l+1)}{r} j_l(kr) P_l^{|m|}(\cos\theta)\vec{e}_r + \left(\frac{\partial}{\partial\theta} P_l^{|m|}(\cos\theta)\vec{e}_\theta + \frac{im}{\sin\theta} P_l^{|m|}(\cos\theta)\vec{e}_\phi \right) \frac{1}{r}\frac{\partial}{\partial r}[rV(r)] \right\} \exp(im\phi), \tag{1b}$$

where $V(r) = Ah_l^{(1)}(kr) + Bh_l^{(2)}(kr)$, A and B are constants, $k = \sqrt{\varepsilon}\,\omega/c$, and the spherical functions $h_l^{(1)}(x)$ and $h_l^{(2)}(x)$ are related to the Hankel functions by $h_l^{(1,2)}(x) = \sqrt{\pi/2x} H_{l+1/2}^{(1,2)}(x)$. $P_l^{|m|}(\cos\theta)$ is an associated Legendre function.

Similarly, for the TM eigenmodes

$$\vec{H}_{l,m} = \varepsilon k_0 \left(\frac{m}{\sin\theta} P_l^{|m|}(\cos\theta)\vec{e}_\theta + i\frac{\partial}{\partial\theta} P_l^{|m|}(\cos\theta)\vec{e}_\phi \right) V(r)\exp(im\phi), \tag{2a}$$

$$\vec{E}_{l,m} = \left\{ \frac{l(l+1)}{r} j_l(kr) P_l^{|m|}(\cos\theta)\vec{e}_r + \left(\frac{\partial}{\partial\theta} P_l^{|m|}(\cos\theta)\vec{e}_\theta + \frac{im}{\sin\theta} P_l^{|m|}(\cos\theta)\vec{e}_\phi \right) \frac{1}{r}\frac{\partial}{\partial r}[rV(r)] \right\} \exp(im\phi). \tag{2b}$$

An electromagnetic field in the central core of the microcavity can be represented as the sum of incoming and outgoing waves. The field at the center of the microcavity should be finite, and this requires, in the case of the empty microcavity, that the incoming and outgoing waves have equal amplitude in the central core and the radial dependence of the field be described by the spherical Bessel function $j_l = [h_l^{(1)}(x) + h_l^{(2)}(x)]/2$. Thus, the electromagnetic field of each eigenmode is described by Eqs. (1) and (2) with $V(r) = j_l(kr)$.

Only in the case of the TM mode with $l=1$ is the electric field of the eigenmode not equal to zero at the center of the SMC. Hence, only with this mode is there significant interaction with a (nonmagnetic) quantum dot placed at the center of the microcavity. For all other cavity modes, the electric field at the center of the SMC vanishes, and there is negligible interaction with a QD placed there.

The electric field of the TM eigenmode of an empty SMC, characterized by $l=1$, $m=0$, has the form

$$\vec{E}^{\text{hom}} = \frac{2}{r} j_1(kr)\cos(\theta)\vec{e}_r - \frac{1}{r}\frac{d}{dr}[rj_1(kr)]\sin\theta\vec{e}_\theta. \tag{3}$$

Using the matrix $\hat{M}$,

$$\hat{M} = \begin{pmatrix} \sin\theta\cos\phi & \cos\theta\cos\phi & -\sin\phi \\ \sin\theta\sin\phi & \cos\theta\sin\phi & \cos\phi \\ \cos\theta & \sin\theta & 0 \end{pmatrix} \tag{4}$$

for the transformation from spherical to Cartesian coordinates, we can represent the electric field in the form

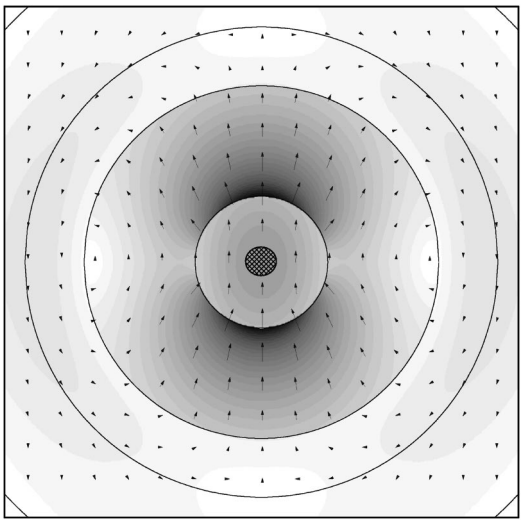

FIG. 2. Schematic distribution of the magnitude of the electric-field intensity in a cross section of the spherical microcavity for the TM mode with $l=1$, $m=0$. The quantum dot is shown in the center of the microcavity as a patterned circle. The gray shading corresponds to the magnitude of the electric field. The magnitude and direction of the electric field are also indicated by arrows.

$$\vec{E}^{\rm hom}=\left(\frac{2}{r}j_1(kr)-\frac{1}{r}\frac{d}{dr}[rj_1(kr)]\right)\cos\theta\sin\theta(\cos\phi\vec{e}_x+\sin\phi\vec{e}_y)+\left(\frac{2}{r}j_1(kr)\cos^2\theta+\frac{1}{r}\frac{d}{dr}[rj_1(kr)]\sin^2\theta\right)\vec{e}_z, \tag{5}$$

from which it follows that the electric field near the center of the SMC is spatially uniform and is directed along the z axis, as illustrated in Fig. 2.

The electromagnetic field in the vicinity of a QD is described by Maxwell's equations with the excitonic contribution to the polarization $\vec{P}(\vec{r})$ taken into account:

$$\nabla\times\nabla\times\vec{E}-\varepsilon k_0^2\vec{E}=4\pi k_0^2\vec{P}(\vec{r}). \tag{6}$$

Here $k_0=\omega/c$ and

$$\vec{P}(\vec{r})=\int\tilde{\chi}(\omega,\vec{r},\vec{r}')\vec{E}(\vec{r})d\vec{r}'. \tag{7}$$

The nonlocal excitonic susceptibility has the form[10]

$$\tilde{\chi}(\omega,\vec{r},\vec{r}')=\chi(\omega)\Phi(\vec{r})\Phi(\vec{r}'), \tag{8}$$

where the function $\Phi(\vec{r})$ is related to the exciton envelope function $\Psi(\vec{r},\vec{r}')$ by $\Phi(\vec{r})=\Psi(\vec{r},\vec{r})$, and

$$\chi(\omega)=\frac{\varepsilon\omega_{LT}a_B^3/4}{\tilde{\omega}_{ex}-\omega-i\Gamma} \tag{9}$$

in terms of the transverse-longitudinal splitting ω_{LT}, the Bohr radius a_B, the resonance frequency $\tilde{\omega}_{\rm ex}$, and the nonradiative damping factor Γ. Further, we shall neglect the complex valence-band structure and apparent short-range and long-range exchange splittings of the exciton-state QD. These effects have been addressed in Ref. 20. In the numerical calculations we shall use the parameters of the heavy-hole exciton resonance in GaAs. An extention of our formalism by taking into account the exciton fine structure is straightforward but requires quite tedious computations. For the exciton ground state in a spherical QD, the wave function $\Phi(\vec{r})$ is spherically symmetric , so $\Phi(\vec{r})=\Phi(r)$. Substituting Eq. (8) into Eq. (7), we can write $\vec{P}(\vec{r})$ as

$$\vec{P}(\vec{r})=\chi(\omega)\Phi(r)\vec{\Lambda}, \tag{10}$$

where $\vec{\Lambda}=\int\Phi(r)\vec{E}(\vec{r})d\vec{r}$.

The solution of Eq. (6) can be found by the Green-function technique:

$$E_\alpha(\vec{r})=E_\alpha^{\rm hom}(\vec{r})+k_0^2\int G_{\alpha\beta}(\vec{r}-\vec{r}')P_\beta(\vec{r}')d\vec{r}', \tag{11}$$

where $\alpha,\beta=x,y,z$ and the Green function, expressed in Cartesian coordinates, has the form

$$G_{\alpha\beta}(\vec{r}-\vec{r}')=4\pi ik\left[\delta_{\alpha\beta}+\frac{1}{k_0^2}\frac{\partial^2}{\partial r_\alpha\partial r_\beta}\right]h_0^{(1)}(k|\vec{r}-\vec{r}'|). \tag{12}$$

Using Eq. (10), we can rewrite Eq. (11) in the form

$$E_\alpha(\vec{r})=E_\alpha^{\rm hom}(\vec{r})+k_0^2\chi(\omega)D_{\alpha\beta}(\vec{r})\Lambda_\beta, \tag{13}$$

where

$$D_{\alpha\beta}=\int G_{\alpha\beta}(\vec{r}-\vec{r}')\Phi(r')d\vec{r}'. \tag{14}$$

Using the relation[21]

$$h_0^{(1)}(k|\vec{r}-\vec{r}'|)=\begin{cases}\sum_{n=0}^{\infty}(2n+1)h_n^{(1)}(kr)j_n(kr')P_n(\cos\theta), & r>r'\\ \sum_{n=0}^{\infty}H_n^{(1)}(kr')j_n(kr)P_n(\cos\theta), & r<r',\end{cases} \tag{15}$$

the matrix $\hat{D}$ can be expressed in the form

$$D_{\alpha\beta}=4\pi ik\int \Phi(r')\left[\delta_{\alpha\beta}+\frac{1}{k_0^2}\frac{\partial^2}{\partial r_\alpha \partial r_\beta}\right] \times\left(\begin{cases}\sum_{n=0}^{\infty}(2n+1)h_n^{(1)}(kr)j_n(kr')P_n(\cos\theta), & r>r' \\ \sum_{n=0}^{\infty}H_n^{(1)}(kr')j_n(kr)P_n(\cos\theta), & r<r'\end{cases}\right)d\vec{r}'. \tag{16}$$

Using the identity $\int_0^\pi P_n(\cos\theta)\sin(\theta')d\theta'=2\delta_{0n}$, one can conclude that only those terms in Eq. (16) that have $n=0$ give nonzero contribution to $D_{\alpha\beta}$, and

$$D_{\alpha\beta}=(4\pi)^2 ik\left[\delta_{\alpha\beta}+\frac{1}{k_0^2}\frac{\partial^2}{\partial r_\alpha \partial r_\beta}\right]S(r), \tag{17}$$

where $S(r)$ depends on the radius only,

$$\begin{aligned}S(r)&=h_0^{(1)}(kr)\int_0^r \Phi(r')j_0(kr')r'^2dr' \\ &\quad+j_0(kr)\int_r^\infty \Phi(r')h_0^{(1)}(kr')r'^2dr' \\ &=j_0(kr)\int_0^\infty \Phi(r')j_0(kr')r'^2dr' \\ &\quad+iy_0(kr)\int_0^r \Phi(r')j_0(kr')r'^2dr' \\ &\quad+ij_0(kr)\int_r^\infty \Phi(r')y_0(kr')r'^2dr'\end{aligned} \tag{18}$$

and can be represented in the form

$$S(r)=\frac{1}{4\pi}[j_0(kr)V_0+iV_1(r)] \tag{19}$$

where $V_0=\int\Phi(r)j_0(kr)d\vec{r}$ and

$$\begin{aligned}V_1(r)=4\pi\Bigg(&y_0(kr)\int_0^r \Phi(r')j_0(kr')r'^2dr' \\ &+j_0(kr)\int_r^\infty \Phi(r')y_0(kr')r'^2dr'\Bigg).\end{aligned}$$

Thus

$$D_{\alpha\beta}=4\pi ik\left[\delta_{\alpha\beta}+\frac{1}{k_0^2}\frac{\partial^2}{\partial r_\alpha \partial r_\beta}\right][j_0(kr)V_0+iV_1(r)]. \tag{20}$$

If r exceeds the size of the exciton wave function, $V_1(r)=V_0y_0(kr)$, $S(r)=(V_0/4\pi)h_0^{(1)}(kr)$, and the matrix $\hat{D}$ can be represented in the form

$$D_{\alpha\beta}=4\pi ik\left[\delta_{\alpha\beta}+\frac{1}{k_0^2}\frac{\partial^2}{\partial r_\alpha \partial r_\beta}\right]h_0^{(1)}(kr). \tag{21}$$

Now, multiplying Eq. (13) by $\Phi(\vec{r})$ and integrating over $\vec{r}$,

$$\begin{aligned}&\int \Phi(\vec{r})E_\alpha(\vec{r})d\vec{r} \\ &\quad=\int \Phi(\vec{r})E_\alpha^{\hom}(\vec{r})d\vec{r}+k_0^2\chi(\omega)\int \Phi(\vec{r})D_{\alpha\beta}(\vec{r})d\vec{r}\Lambda_\beta.\end{aligned} \tag{22}$$

The integral on the left side of the equation is just $\vec{\Lambda}$. Making use of the identities

$$\frac{1}{r}\frac{d}{dr}[rj_1(kr)]=kj_0(kr)-\frac{j_1(kr)}{r}, \tag{23a}$$

$$\int_0^\pi \sin^3\theta\,d\theta=\frac{4}{3}, \tag{23b}$$

$$\int_0^\pi \cos^2\theta\sin\theta\,d\theta=\frac{2}{3}, \tag{23c}$$

and Eq. (5), one can show that

$$\int \vec{E}^{\hom}\Phi(r)dr=\frac{2}{3}kV_0\vec{e}_z. \tag{24}$$

Taking into account the spherical symmetry of the functions $\Phi(\vec{r})$ and $S(\vec{r})$, we conclude that the integral $\int\Phi(\vec{r})[\delta_{\alpha\beta}+(1/k_0^2)(\partial^2/\partial r_\alpha\partial r_\beta)]S(\vec{r})d\vec{r}$ vanishes if $\alpha\neq\beta$, so that we can rewrite Eq. (22) in the form

$$\Lambda\vec{e}_z=\tfrac{2}{3}kV_0\vec{e}_z+k_0^2\chi W\Lambda\vec{e}_z, \tag{25}$$

where $W=\int\Phi(\vec{r})D_{zz}d\vec{r}$. It is apparent that the presence of the quantum dot does not affect the direction of the electric field of the eigenmode near the QD, and the resulting polariton state is threefold-degenerate. Equation (25) yields

$$\Lambda=\frac{2/3kV_0}{1-k_0^2\chi W}. \tag{26}$$

Using the identity (23a), we can rewrite Eq. (17) in the form

$$\begin{aligned}D_{\alpha\beta}=4\pi ik\Bigg\{V_0\Bigg[&\left(3\frac{j_1(kr)}{r}-kj_0(kr)\right)\frac{r_\alpha r_\beta}{r^2}+\delta_{\alpha\beta} \\ &+\left(kj_0(kr)-\frac{j_1(kr)}{r}\right)\Bigg]+i\left[\delta_{\alpha\beta}+\frac{1}{k_0^2}\frac{\partial^2}{\partial r_\alpha\partial r_\beta}\right]P(r)\Bigg\}.\end{aligned} \tag{27}$$

In particular,

$$D_{zz}=4\pi ikV_0\left[\left(3\frac{j_1(kr)}{r}-kj_0(kr)\right)\cos^2\theta+\left(kj_0(kr)-\frac{j_1(kr)}{r}\right)\right]-4\pi k\left[P(r)+\frac{\sin^2\theta}{k_0^2}\frac{\partial P(r)}{\partial r}+\frac{\cos^2\theta}{k_0^2}\frac{\partial^2 P(r)}{\partial r^2}\right], \tag{28}$$

from which it follows that

$$W=\tfrac{8}{3}\pi ik^2V_0^2-4\pi kQ, \tag{29}$$

where

$$Q=\int \Phi(r)\left[P(r)+\frac{\sin^2\theta}{k_0^2}\frac{\partial P(r)}{\partial r}+\frac{\cos^2\theta}{k_0^2}\frac{\partial^2 P(r)}{\partial r^2}\right]d\vec{r}.$$

We can rewrite Eq. (13) in spherical coordinates using the matrix $\hat{\tilde{D}}=\hat{M}^{-1}\hat{D}$:

$$E_{\alpha\beta}(\vec{r})=E_{\mathrm{hom}}(\vec{r})+k_0^2\chi(\omega)\tilde{D}_{\alpha\beta}(\vec{r})\Lambda_\beta. \tag{30}$$

At the large distance from the QD,

$$\tilde{D}_{rz}=\frac{8\pi ikV_0}{r}h_1^{(1)}(kr)\cos\theta, \tag{31a}$$

$$\tilde{D}_{\theta z}=-\frac{4\pi ikV_0}{r}\frac{d}{dr}[rh_1^{(1)}(kr)]\sin\theta, \tag{31b}$$

$$\tilde{D}_{\phi z}=0, \tag{31c}$$

and we obtain the result that

$$\vec{E}(\vec{r})=\vec{E}^{\mathrm{hom}}(\vec{r})+k_0^2\chi(\omega)(\tilde{D}_{rz}\vec{e}_r+\tilde{D}_{\theta z}\vec{e}_\theta)\Lambda. \tag{32}$$

Substituting Eqs. (3) and (28) into Eq. (30), we can obtain the electric field

$$\vec{E}(\vec{r})=\frac{1}{r}h_1^{(2)}(kr)\cos\theta\vec{e}_r-\frac{1}{2r}\frac{d}{dr}[rh_1^{(2)}(kr)]\sin\theta\vec{e}_\theta+[1+8\pi ikk_0^2\chi(\omega)V_0\Lambda]\times\left(\frac{1}{r}h_1^{(1)}(kr)\cos\theta\vec{e}_r--\frac{1}{2r}\frac{d}{dr}[rh_1^{(2)}(kr)]\sin\theta\vec{e}_\theta\right). \tag{33}$$

Considering the field as the superposition of the converging (incident) and diverging (reflected from QD) spherical waves, we can obtain the amplitude reflection coefficient of the spherical wave incident on the QD as

$$r_{\mathrm{QD}}=[1+8\pi ikk_0^2\chi(\omega)V_0\Lambda]. \tag{34}$$

Substituting Eqs. (9), (26), and (29) into Eq. (34), we can obtain the reflection coefficient in the form

$$r_{\mathrm{QD}}=1+\frac{2i\Gamma_0}{\omega_{\mathrm{ex}}-\omega-i(\Gamma+\Gamma_0)}, \tag{35}$$

where the radiative damping factor

$$\Gamma_0=\tfrac{2}{3}\pi k^4V_0^2\omega_{LT}a_B^3 \tag{36}$$

and renormalized resonance frequency

$$\omega_{\mathrm{ex}}=\tilde{\omega}_{\mathrm{ex}}+\pi Q\omega_{LT}k^3a_B^3. \tag{37}$$

When a converging spherical wave reaches the center of the microcavity, it becomes a diverging wave, contributing to the reflection coefficient. It follows that the absorption and reflection coefficients are related by

$$A=1-|r_{\mathrm{QD}}|^2. \tag{38}$$

B. Eigenmodes of a spherical microcavity with an embedded quantum dot

The radial dependence of the tangential components of the *magnetic* [which in the case of TM polarization is described by Eq. 2(a)] field in a central core containing a quantum dot located at the center of the SMC can be written in the form

$$H(r)=h_1^{(2)}(kr)+r_{\mathrm{QD}}h_1^{(1)}(kr) \tag{39}$$

and can be represented as a two-dimensional vector $(h_1^{(2)}(kr),r_{\mathrm{QD}}h_1^{(1)}(kr))$, whose components are the magnitudes of the converging and diverging waves. At the boundary of the central sphere in Fig. 1, which has the radius R_0, the ratio of the amplitudes of the converging and diverging waves is given by the reflection coefficient r_B of the spherical Bragg mirror, which provides the optical confinement in the structure, and the magnetic field can be represented as $C(r_B,1)$, where C is a constant. The equation defining the frequencies of the eigenmodes of the SMC with an embedded quantum dot can be obtained by equating the two vectors defined above, to give

$$h_1^{(2)}(kR_0)=r_{\mathrm{BR}}r_{\mathrm{QD}}h_1^{(1)}(kR_0). \tag{40}$$

In the case of negligible absorption of light in the dot, Eq. (40) can be reduced to

$$\arg(h_1^{(2)}(kR_0))-\arg(h_1^{(1)}(kR_0))-\arg(r_{\mathrm{BR}})-\arg(r_{\mathrm{QD}})=2\pi N. \tag{41}$$

The amplitude reflection coefficient of a QD can be represented in the form

$$r_{\mathrm{QW}}=\frac{(\omega_{\mathrm{ex}}-\omega)^2+(\Gamma^2-\Gamma_0^2)+i2\Gamma_0(\omega_{\mathrm{ex}}-\omega)}{(\omega_{\mathrm{ex}}-\omega)^2+(\Gamma+\Gamma_0)^2}. \tag{42}$$

Let us assume that the frequencies of the exciton polariton are sufficiently different from the resonance frequency ω_{ex} (this is the case in planar and cylindrical microcavities in the

strong-coupling regime) so $(\Gamma+\Gamma_0)\ll|\omega_{ex}-\omega|$. In this case, the phase of r_{QD} is given to a good approximation by

$$\arg(r_{QW})\cong\frac{2\Gamma_0}{(\omega_{ex}-\omega_{em})}. \tag{43}$$

When the central core radius exceeds the wavelength of the light, the spherical function can be approximated by their asymptotic values, which gives $\arg(h_1^{(1)}(kR_0))-\arg(h_1^{(2)}(kR_0))\approx\pi+2kR_0$, and the phase of the reflection coefficient of the Bragg reflector can be approximated by the expression

$$\arg(r_{BR})\approx b\frac{\omega-\omega_b}{\omega_b}, \tag{44}$$

where[12] $b=\pi n_1 n_2/\sqrt{\varepsilon}(n_2-n_1)$, and allows us to rewrite Eq. (41) in the form

$$\pi+b\frac{\omega-\omega_b}{\omega_b}-\frac{2\Gamma_0}{\omega-\omega_{ex}}+2\frac{\omega}{c}\sqrt{\varepsilon}R_0=2\pi N. \tag{45}$$

Since the frequency of the TM eigenmode with $l=1$ of an empty SMC is given by

$$\omega_N=\frac{\omega_b[\pi(2N+1)+b]}{b+2\dfrac{R_0}{c}\sqrt{\varepsilon}\omega_b}, \tag{46}$$

we can rewrite Eq. (45) in the form

$$(\omega-\omega_N)(\omega-\omega_{ex})=(\Delta/2)^2, \tag{47}$$

where the value of the splitting is

$$\Delta=2\sqrt{\frac{2\Gamma_0\omega_b}{b+2\dfrac{R_0}{c}\sqrt{\varepsilon}\omega_b}}. \tag{48}$$

Finally, the frequencies of the exciton polaritons are given by

$$\omega=\frac{\omega_N+\omega_{ex}}{2}\pm\frac{\sqrt{(\omega_N-\omega_{ex})^2+4\delta^2}}{2}. \tag{49}$$

III. RESULTS AND DISCUSSONS

Figure 3 shows the spectral dependence of the absorption coefficient for a spherical electromagnetic wave with $l=1$ incident on a quantum dot with different values of the nonradiative damping Γ. Note that in the case $\Gamma=0$, the magnitude of the absorption coefficient is zero, which is quite natural since in this case there is no dissipation of energy. The magnitude of the diverging wave is the same as the magnitude of the converging wave in this case, while its initial phase is modified according to Eqs. (42) and (43). As Γ increases, the peak value of the absorption coefficient, which corresponds to the exciton resonance frequency $\omega=\omega_{ex}$, increases and reaches unity when the nonradiative and radiative damping are equal $(\Gamma=\Gamma_0)$, as shown in the inset in Fig. 3. Further increase of Γ leads to a decrease of the peak

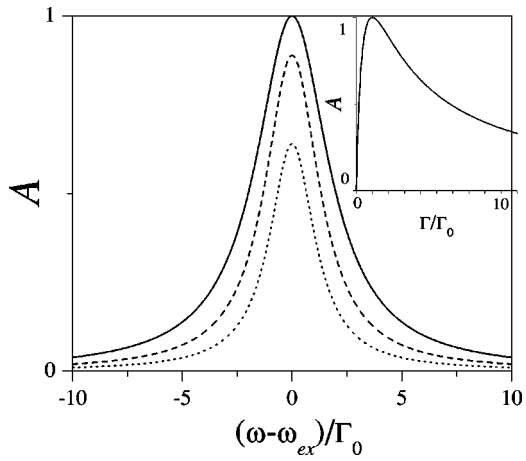

FIG. 3. Spectral dependence of the absorption coefficient of a spherical TM converging wave with $l=1$, $m=0$ incident on a quantum dot calculated for different values of the nonradiative damping Γ: solid line, $\Gamma=\Gamma_0$; dashed line, $\Gamma=1/2\Gamma_0$; dotted line, $\Gamma=1/4\Gamma_0$. The inset shows the reflection coefficient at the resonant frequency as a function of the nonradiative damping factor Γ .

value of the absorption coefficient and a broadening of the absorption line. Similar behavior has been found recently in the case of a cylindrical light wave incident on a quantum wire.[22] The latter can be understood by taking into account the fact that the systems have either a point or line where the converging wave diverges (and vice versa).

The interaction between localized exciton and photon modes has two different regimes, namely the strong-coupling regime, which holds when the splitting of the modes exceeds the half-sum of their damping parameters and two peaks can be distinguished in the absorption spectrum, and the weak-coupling regime, which holds when the half-sum of the damping parameters exceeds the splitting and the two peaks in the absorption spectra merge into one. In the case of a realistic quantum well or quantum wire exciton, the nonradiative damping of the exciton is usually much larger than the radiative one. This is because the acoustic phonon scattering of excitons is quite efficient within continuous energy bands. In contrast, quantum dots possess a discrete energy spectrum. Therefore, the nonradiative damping of a quantum dot exciton is very small, and comparable with the radiative damping.[23] Experimentally, the emission linewidth of a quantum dot exciton is difficult to measure directly, often being less than the spectral resolution of the current equipment.[24] Therefore, the lifetime of the zero-dimensional polariton in this case is governed by the quality factor (Q factor) of the spherical Bragg microcavity.

Figure 4 shows the absorption spectra, calculated using the transfer matrix method, of a SMC formed by a central core of refractive index 2.7 and a seven-period spherical Bragg reflector, with layers of refractive indices 1.45 and 2.7. Results for different values of the central core radius are shown. The refractive indices correspond to those for ZnTe and SiO_2, which are the materials whose layers can be deposited by means of colloidal chemistry.[16,17]. The parameters of the QD are chosen to be similar to those for realistic QDs based on a II-VI semiconductor compound: $\Gamma_0=2$

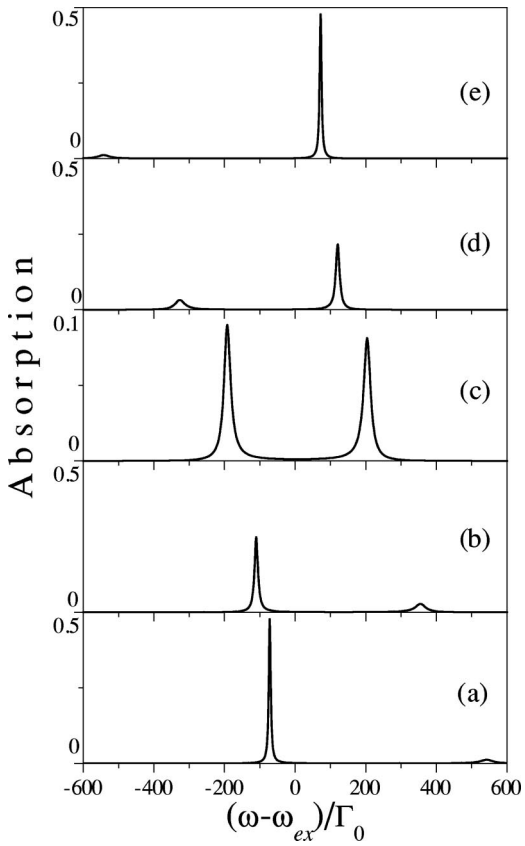

FIG. 4. Absorption spectra in the strong-coupling regime of a spherical microcavity comprising a central core and a seven-period-thick Bragg reflector. The five spectra relate to different values of the central core radius R_0; (a) $R_0\omega_{ex}/2\pi c=0.102\,65$; (b) $R_0\omega_{ex}/2\pi c=0.1028$; (c) $R_0\omega_{ex}/2\pi c=0.102\,955$; (d) $R_0\omega_{ex}/2\pi c=0.1031$; (e) $R_0\omega_{ex}/2\pi c=0.103\,25$. The values of the radiative and nonradiative damping are $\Gamma_0=2\times10^{-6}\omega_{ex}$, $\Gamma=10^{-6}\omega_{ex}$.

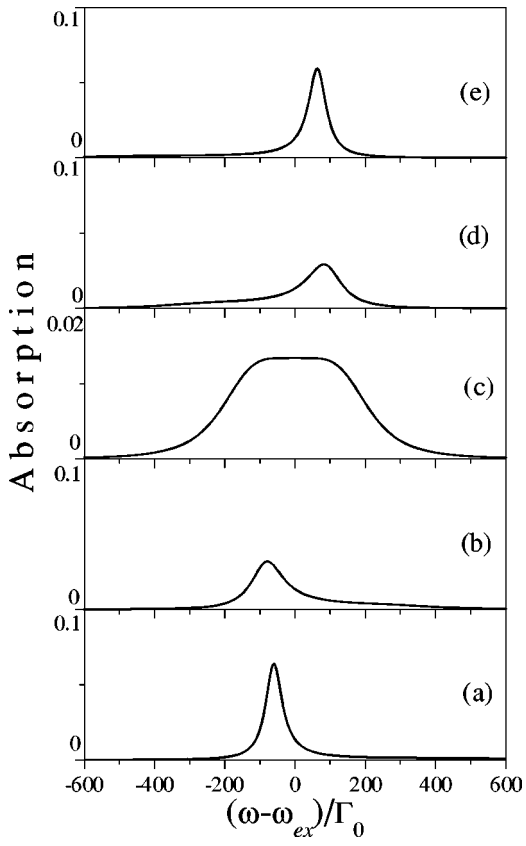

FIG. 5. Absorption spectra in the weak-coupling regime of a spherical microcavity comprising a central core and a five-period-thick Bragg reflector. The five spectra relate to different values of the central core radius R_0; (a)$R_0\omega_{ex}/2\pi c=0.102\,65$; (b) $R_0\omega_{ex}/2\pi c=0.1028$; (c) $R_0\omega_{ex}/2\pi c=0.102\,955$; (d) $R_0\omega_{ex}/2\pi c=0.1031$; (e) $R_0\omega_{ex}/2\pi c=0.103\,25$. The values of radiative and nonradiative damping are $\Gamma_0=2\times10^{-6}\omega_{ex}$, $\Gamma=10^{-6}\omega_{ex}$.

$\times10^{-6}\omega_{ex}$, $\Gamma=10^{-6}\omega_{ex}$. Increasing the central core radius reduces the frequency of the eigenmode of the empty cavity. When a cavity mode is detuned from the exciton resonance, the spectrum exhibits a well pronounced peak, corresponding to an excitonic transition and a small peak corresponding to the uncoupled cavity mode [see the curves of Figs. 4(a) and 4(e)]. Tuning the optical mode towards the exciton resonance leads to a shift of both peaks, which exhibit identical shapes in the case of precise tuning [Fig. 4(c)]. The splitting of the cavity mode corresponds to the value of the vacuum Rabi splitting Δ given by Eq. (48). This behavior of the absorption spectrum as a function of detuning is a signature of the strong-coupling regime. The first theoretical proof of the possibility of strong coupling of quantum dot excitons with cavity photons has been given by Andreani *et al.*[14] The present analysis of the eigenmodes of a spherical microcavity confirms those predictions.

Decreasing the number of layers in the Bragg reflector of the cavity reduces the Q factor of the cavity and leads to a broadening of the cavity mode. Figure 5 shows the absorption spectra of the SMC with a QD and a reflector consisting of five pairs of layers. In this case, the width of the cavity mode exceeds the splitting. When the cavity mode is detuned from the exciton resonance, the absorption peak is asymmetric. Tuning the cavity mode towards the exciton resonance leads to a shift and broadening of the peak as shown in Fig. 6, but the camelback structure does not appear. In the case of precise tuning, the position of the peak in the absorption spectrum corresponds to the exciton resonance frequency, while its width corresponds to the value of Rabi splitting. These spectral features are typical of the weak-coupling regime. Excitons in single quantum dots are subject to the Fermi exclusion principle, and thus only two optically active excitons are allowed in each quantum confined state. Nevertheless, the excitonic transition in a QD has enough oscillator strength to exhibit strong coupling with a spherical cavity mode, as we have shown here.

One can see that in zero-dimensional microcavities with quantum dots, the vacuum field Rabi splitting has essentially the same order of magnitude as in one-dimensional cavities with quantum wires and two-dimensional cavities with quantum wells. Thus, the coupling constant of the exciton to the cavity photon is only weakly influenced by the dimensionality. On the other hand, the threshold to the nonlinear regime takes place at drastically different pumping intensities in the systems of different dimensionalities. In quantum wells, the

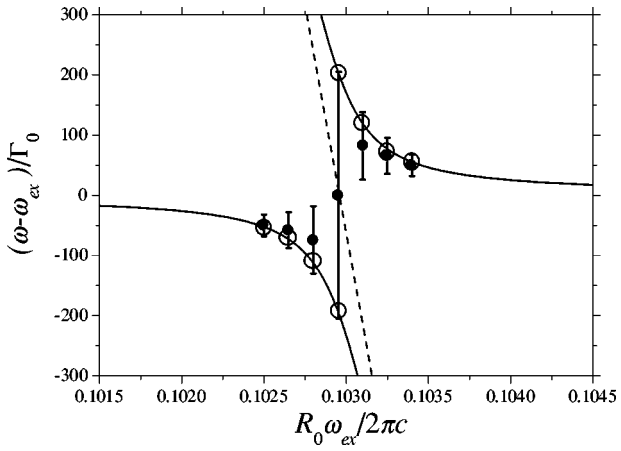

FIG. 6. Dependence on the core radius R_0 of the eigenmode frequencies of the microcavity with an embedded quantum dot obtained by solving Eq. (41) (shown by solid lines), compared with the positions of the peaks in the absorption spectra in the strong-coupling regime (open circles) and weak-coupling regime (solid circles). The vertical bars indicate the width of the absorption peak in the weak-coupling regime. The dashed line shows the corresponding dependence for the empty microcavity. The values of the radiative and nonradiative damping are $\Gamma_0=2\times10^{-6}\omega_{\rm ex}$, $\Gamma=10^{-6}\omega_{\rm ex}$.

concentration of about 10^{11} electrons is needed to screen the free-exciton resonance and to make the biexciton resonance visible. On the other hand, in a zero-dimensional microcavity with a single quantum dot, the creation of only two electron-hole pairs causes already the nonlinear phenomena, and the biexciton can be formed. This peculiar behavior could have a substantial influence on the optical properties of microcavities.[25] In particular, this effect could lead to the sublinear dependence of the intensity of light emission from a microcavity in a zero-dimensional case.

Finally, we should point out that by varying the parameters of the system, we can change the splitting of the zero-dimensional polariton states. Thus, a SMC with a QD provides an opportunity for quantum state engineering, which could be interesting from the point of view of the experimental implementation of a quantum computer.[26]

IV. CONCLUSION

The interaction of zero-dimensional excitons and photons has been analyzed theoretically using the theory of nonlocal dielectric response and the transfer matrix method. Light absorption by a single quantum dot has been analyzed and it is shown that the resonant excitonic absorption of the $l=1$ TM spherical wave incident on the quantum dot is total when the nonradiative and radiative damping factors of the exciton are equal. An equation for the eigenenergies and an expression for the value of the vacuum Rabi splitting for the zero-dimensional polariton have also been obtained. Absorption spectra for a specific type of structure have been obtained and the transition between the strong- and weak-coupling regime has been illustrated.

ACKNOWLEDGMENTS

The work was partly funded by EPSRC research Grant GL/R 73258 and 73159, by European Commission, project IST-1999-19009 PHOBOS, and partly by INTAS 928 and RFBR. M.V.M. thanks the A. von Humboldt Foundation.

[1] J.J. Hopfield, Phys. Rev. **112**, 1555 (1958).
[2] V.M. Agranovich, Zh. Éksp. Teor. Fiz. **37**, 430 (1959) [Sov. Phys. JETP **37**, 307 (1960)].
[3] V.A. Kiselev, I.N. Uraltsev, and B.S. Razbirin, Pisma Zh. Éksp. Teor. Fiz. **18**, 504 (1973) [JETP Lett. **18**, 296 (1973)].
[4] D. Frohlich, A. Kulik, B. Uebbing, A. Mysyrowicz, V. Langer, H. Stolz, and W. von der Osten, Phys. Rev. Lett. **67**, 2343 (1991).
[5] L.C. Andreani, F. Tassone, and F. Bassani, Solid State Commun. **77**, 641 (1991).
[6] E.L. Ivchenko, Fiz. Tverd. Tela (Leningrod) **33**, 2388 (1991) [Sov. Phys. Solid State **33**, 1344 (1991)].
[7] M. Sugasaki, H.W. Ren, S.V. Nair, K. Nishi, S. Sugou, T. Okuna, and Y. Masumoto, Phys. Rev. B **59**, R5300 (1999).
[8] M. Bayer, A. Kuther, A. Forchel, A. Gorbunov, V.B. Timofeev, F. Schofer, J.P. Reithmaier, T.L. Rienecke, and S.N. Walk, Phys. Rev. Lett. **82**, 1748 (1999).
[9] E.L. Ivchenko and A.V. Kavokin, Fiz. Tverd. Tela. (Leningrad) **34**, 1815 (1992) [Sov. Phys. Solid State **34**, 1815 (1992)].
[10] L. Banyai and S.W. Koch, *Semiconductor Quantum Dots* (World Scientific, Singapore, 1993).
[11] C. Weisbuch, M. Nishioka, A. Ishikawa, and Y. Arakawa, Phys. Rev. Lett. **69**, 3314 (1992).
[12] E.L. Ivchenko, M.A. Kaliteevski, A.V. Kavokin, and A.I. Nesvizhskii, J. Opt. Soc. Am. B **13**, 1061 (1996).
[13] J.M. Grard, B. Sermage, B. Gayral, B. Legrand, E. Costard, and V. Thierry-Mieg, Phys. Rev. Lett. **81**, 1110 (1998).
[14] L.C. Andreani, G. Panzarini, and J.M. Gerard, Phys. Rev. B **60**, 13 276 (1999).
[15] M.A. Kaliteevski, R.A. Abram, S. Brand, and V.V. Nikolaev, Phys. Status Solidi A **183**, 183 (2001); J. Mod. Opt. **48**, 1503 (2001).
[16] T. Rajh, O.I. Micic, and A.J. Nozhik, J. Phys. Chem. **97**, 11 999 (1993).
[17] Yu.A. Vlasov, V.N. Astratov, O.Z. Karimov, A.A. Kaplianskii, V.N. Bogomolov, and A.V. Prokofiev, Phys. Rev. B **55**, R13 791 (1997).
[18] M.V. Artemyev and U. Woggon, Appl. Phys. Lett. **76**, 1353 (2000).
[19] D. S. Jones, *The Theory of Electromagnetism* (Pergamon, London, 1964), p. 483; W. K. H. Panovsky and M. Phillips, *Classical Electricity and Magnetism* (Addison-Wesley, London, 1962), p. 233; J. J. Jackson, *Classical Electrodynamics* (Wiley, New York 1999), p. 95.
[20] S.V. Gupalov, E.L. Ivchenko, and A.V. Kavokin, Zh. Éksp. Teor.

Fiz. **113**, 703 (1998) [JETP **86**, 388 (1998)].

[21] G. A. Korn and T. M. Korn, *Mathematical Handbook for Scientists and Engineers : Definitions, Theorems and Formulas for Reference and Review* (McGraw-Hill, New York, 1961), Chap. 21.8-13, formulas 21.8-73.

[22] M.A. Kaliteevski, S. Brand, R.A. Abram, V.V. Nikolaev, M.V. Maximov, N.N. Ledentsov, C.M. Sotomayor-Torres, and A.V. Kavokin, Phys. Rev. B **61**, 13 791 (2000).

[23] D. Gammon, E.S. Snow, B.V. Shanabrook, D.S. Katzer, and D. Park, Phys. Rev. Lett. **76**, 3005 (1996).

[24] M. Grundmann, J. Christen, N.N. Ledentsov, J. Bohrer, D. Bimberg, S.S. Ruvimov, P. Werner, U. Richter, U. Gosele, J. Heidenreich, V.M. Ustinov, A.Y. Egorov, A.E. Zhukov, P.S. Kop'ev, and Z.I. Alferov, Phys. Rev. Lett. **74**, 4043 (1995).

[25] E. Dekel, D. Gershoni, E. Ehrenfreund, D. Spektor, J.M. Garcia, and P.M. Petroff, Phys. Rev. Lett. **80**, 4991 (1998).

[26] A. Imamoglu, D.D. Awshalom, G. Burkard, D.P. DiVincenzo, D. Loss, M. Sherwin, and A. Small, Phys. Rev. Lett. **83**, 4204 (1999).